A Conserved Ribosomal Protein Has Entirely Dissimilar Structures in Different Organisms

Léon Schierholz,[1,†] Charlotte R. Brown,[2,†] Karla Helena-Bueno ,[2,†] Vladimir N. Uversky,[3] Robert P. Hirt ,[2] Jonas Barandun ,[1,*] and Sergey V. Melnikov [2,*]

[1]Department of Molecular Biology, Laboratory for Molecular Infection Medicine Sweden, Umeå Centre for Microbial Research, Science for Life Laboratory, Umeå University, Umeå 901 87, Sweden

[2]Biosciences Institute, Newcastle University School of Medicine, Newcastle upon Tyne NE2 4HH, UK

[3]Department of Molecular Medicine and USF Health Byrd Alzheimer's Research Institute, Morsani College of Medicine, University of South Florida, Tampa, FL 33612, USA

[†]These authors contributed equally to this work.

***Corresponding authors:** E-mails: jonas.barandun@umu.se; sergey.melnikov@ncl.ac.uk.

Associate editor: Xuhua Xia

Abstract

Ribosomes from different species can markedly differ in their composition by including dozens of ribosomal proteins that are unique to specific lineages but absent in others. However, it remains unknown how ribosomes acquire new proteins throughout evolution. Here, to help answer this question, we describe the evolution of the ribosomal protein msL1/msL2 that was recently found in ribosomes from the parasitic microorganism clade, microsporidia. We show that this protein has a conserved location in the ribosome but entirely dissimilar structures in different organisms: in each of the analyzed species, msL1/msL2 exhibits an altered secondary structure, an inverted orientation of the N-termini and C-termini on the ribosomal binding surface, and a completely transformed 3D fold. We then show that this fold switching is likely caused by changes in the ribosomal msL1/msL2-binding site, specifically, by variations in rRNA. These observations allow us to infer an evolutionary scenario in which a small, positively charged, de novo-born unfolded protein was first captured by rRNA to become part of the ribosome and subsequently underwent complete fold switching to optimize its binding to its evolving ribosomal binding site. Overall, our work provides a striking example of how a protein can switch its fold in the context of a complex biological assembly, while retaining its specificity for its molecular partner. This finding will help us better understand the origin and evolution of new protein components of complex molecular assemblies—thereby enhancing our ability to engineer biological molecules, identify protein homologs, and peer into the history of life on Earth.

Graphical abstract

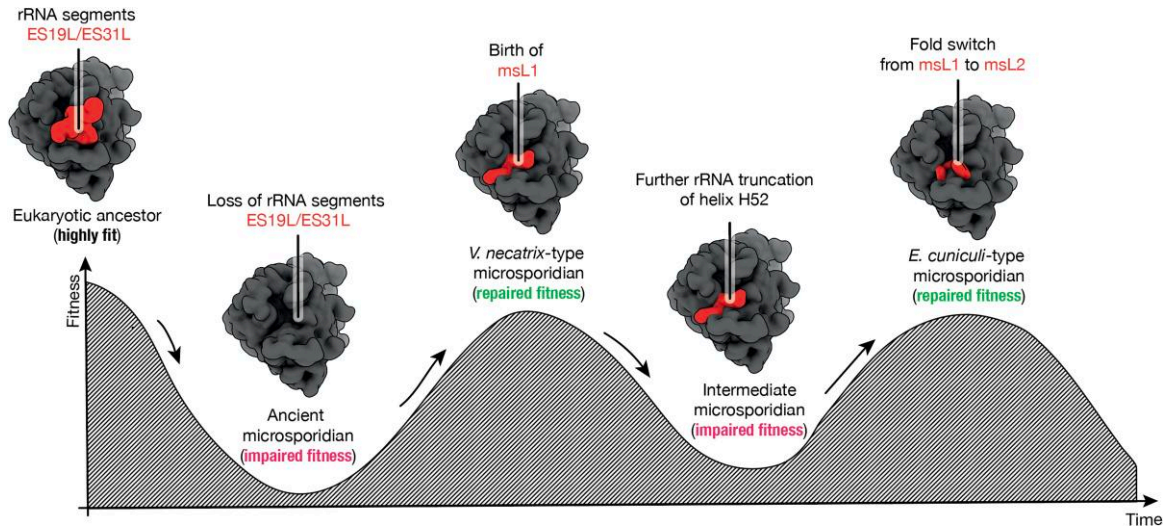

Key words: **ribosome evolution, fold-switching protein, ribosomal protein, microsporidia.**

Received: August 07, 2023. **Revised:** October 23, 2023. **Accepted:** November 16, 2023

Introduction

Because ribosomes are present in every organism and are thought to have originated over 3.9 billion years ago, at the very dawn of life, their structures are widely used to gain insights into past events that are irreparably lost to our direct observations (Bowman et al. 2020). Some of these events include the origin of species (Woese and Fox 1977; Schmidt and Relman 1994; Fox et al. 2012; Petrov et al. 2015), the rise of catalytic RNAs (Fox et al. 2012; Bose et al. 2022), the origin of the genetic code and protein chirality (Fox 2010; Polikanov et al. 2015; Melnikov et al. 2019), as well as adaptations of biological molecules to cellular compartmentalization (Melnikov et al. 2015, 2020) or new environments (Di Giulio 2003; Khachane et al. 2005; Wang et al. 2006; Kimura et al. 2007, 2013; Hu and Lercher 2021; Hu et al. 2022). Studying these evolutionary processes is important beyond genuine curiosity to understand the events that gave rise to our species, along with other eukaryotes; this knowledge is also essential for synthetic biology to help improve natural enzymes or engineer new life from scratch.

Many principles of the molecular evolution of ribosomes have been revealed through the determination of their atomic structures. These structures revealed, for example, that the ribosome's enzymatic core consists of an RNA dimer, hinting at a dimeric primordial RNA as the ribosome ancestor (Belousoff et al. 2010). Later, the discovery of RNA folding mechanisms allowed us to infer the order of events that transformed a relatively small primordial rRNA into one of the most complex molecular assemblies observed in living cells today (Bokov and Steinberg 2009; Petrov et al. 2014).

While structural studies of ribosomes have made it possible to infer the origin, evolution, and functional specialization of rRNA across species, we know little about the origin of ribosomal proteins. If we compare, for example, ribosomes in *Escherichia coli* and humans, we find that they share a set of 33 conserved proteins. However, in addition, these ribosomes contain an array of seemingly unrelated proteins, including 21 bacteria-specific proteins in *E. coli* and 47 archaeo-eukaryotic proteins in humans (Melnikov et al. 2012), with many of these proteins performing essential roles in protein synthesis.

Despite this strikingly dissimilar protein content, the process by which ribosomes acquire and adapt new proteins in different species remains unknown (Kovacs et al. 2017; Alvarez-Carreno et al. 2021, 2022). Did lineage-specific ribosomal proteins first emerge as primitive peptides that gradually transformed into globular proteins? Or did ribosomes capture existing globular proteins through a gain-of-function event? How do these proteins change and coevolve with ribosomes throughout evolutionary time? While these are huge and complicated questions that cannot be comprehensively addressed in any single study, an analysis of ribosome structures and sequences from different organisms can shine light on possible evolutionary scenarios.

Recently, an unexpected opportunity to explore these questions arose from structural studies of ribosomes from the group of fungal parasites known as microsporidia (Barandun et al. 2019; Ehrenbolger et al. 2020; Nicholson et al. 2022). These studies revealed that microsporidian ribosomes possess a unique ribosomal protein, msL1/msL2, which appears to compensate for the rRNA size reduction in microsporidian species. Compared with other studied eukaryotes, most microsporidian species possess severely truncated rRNA, which is devoid of the characteristic rRNA expansion segments that distinguish eukaryotes from bacteria. Also, microsporidians have truncations in most ribosomal proteins (Barandun et al. 2019; Ehrenbolger et al. 2020; Nicholson et al. 2022). Proteins msL1/msL2 appear to compensate for some of these truncations, including the absence of the N-terminus of protein uL23 and the loss of rRNA expansion segments ES19 and ES31 in the 25S rRNA: msL1/msL2 fill the voids in the truncated ribosome structure, mimicking the N-terminus of uL23 and also maintaining contacts between rRNA and ribosomal proteins that are supported by ES19 and ES31 in other eukaryotic ribosomes. Therefore, the presence of msL1/msL2 likely allows microsporidia to maintain normal ribosome biogenesis despite truncations in ribosomal proteins and rRNA.

First discovered in the parasite *Vairimorpha necatrix*, this protein was annotated as msL1-*Vn*; its homologs were subsequently found in 10 microsporidian species, including the parasite *Encephalitozoon cuniculi* (Barandun et al. 2019; Nicholson et al. 2022). Later, however, an investigation of the structure of *E. cuniculi* ribosomes revealed that the msL1-*Vn*–binding site was occupied by a structurally dissimilar protein, which was annotated as msL2-*Ec* (Nicholson et al. 2022). The study of *E. cuniculi* ribosomes, however, has overlooked that the proteins msL1-*Vn* and msL2-*Ec* were previously described as distant homologs following an iterative search of msL1-*Vn* homologs (Barandun et al. 2019). This homology was easy to overlook because msL1-*Vn* and msL2-*Ec* have highly dissimilar structures, with a root mean square deviation (RMSD) of ∼11.4 Å between their backbone residues, compared with a typical RMSD of <2.4 Å for close homologs and ∼4.5 Å for highly distant homologs.

Here, we describe this structural anomaly, in which a seemingly conserved ribosomal protein has completely transformed its 3D structure in one species relative to another. We provide evolutionary insight into the mechanism of this structural shift, likely driven by its adaptation to rRNA reduction in microsporidian parasites. Furthermore, we show that while msL1-*Vn* and msL2-*Ec* share 41% sequence similarity, their conserved residues form dissimilar contacts with the *E. cuniculi* and *V. necatrix* ribosomes. Thus, despite being classified as homologs based on canonical sequence analysis and binding to the same ribosomal helix H52, msL1-*Vn* and msL2-*Ec* have entirely dissimilar 3D structures, binding orientations, and binding modes to the ribosome.

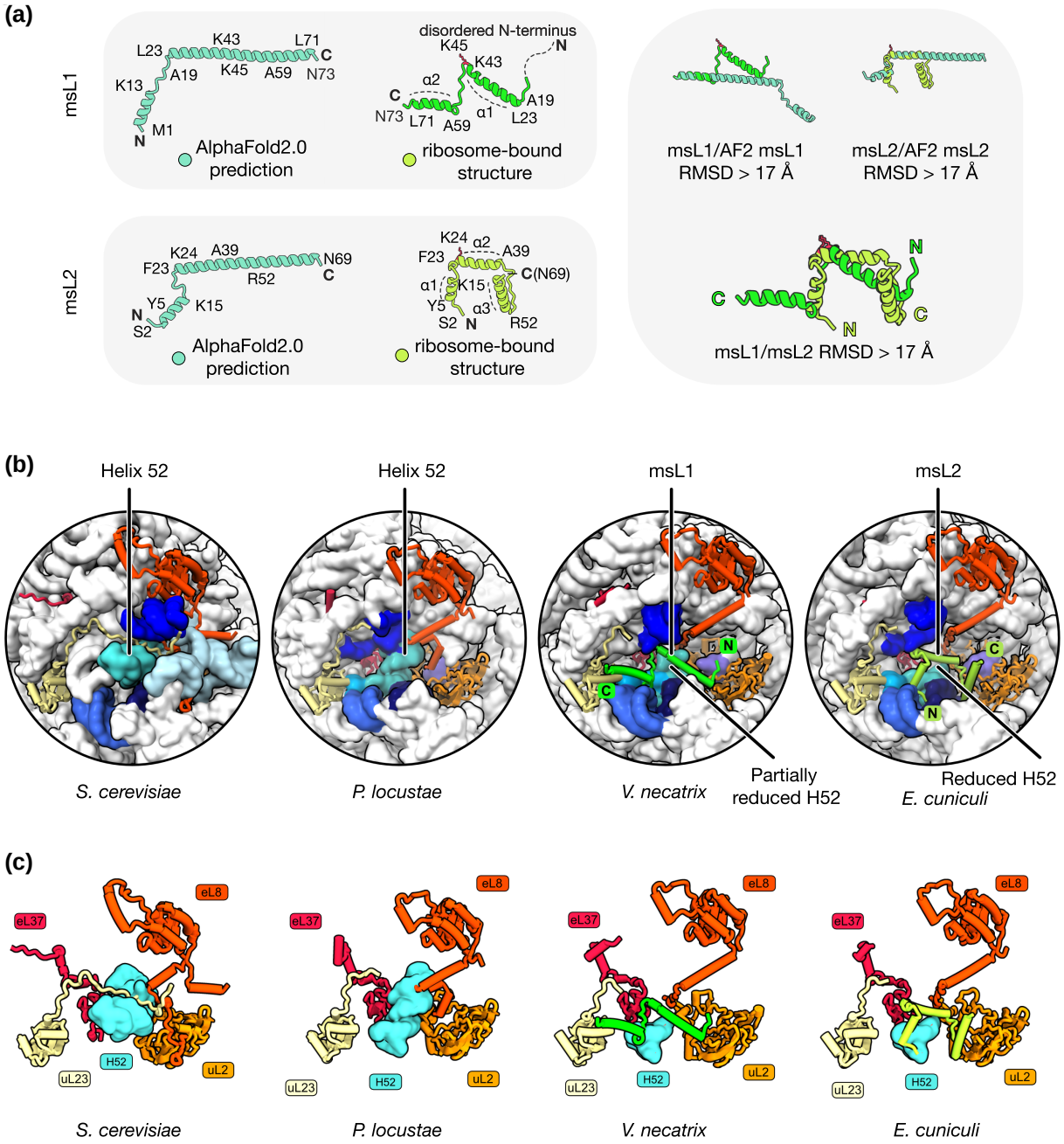

Fig. 1. The msL1/msL2 fold switching in microsporidian ribosomes. a) The left panels compare the structures of 2 homologous ribosomal proteins, msL1-*Vn* and msL2-*Ec*, as predicted by AlphaFold2 (labeled as "AlphaFold2.0 prediction") or observed in the structures of *V. necatrix* and *E. cuniculi* ribosomes (labeled as "ribosome-bound structure"), respectively. The right panels show the superpositions between the AlphaFold2-predicted and experimentally determined structures of msL1-*Vn* and msL2-*Ec* as well as the superposition of the experimentally determined structures of msL1-*Vc* and msL2-*Ec* between each other, providing the RMSD values for each of these superpositions. b) Zoom-in views of ribosome structures compare the binding sites for msL1-*Vc* and msL2-*Ec* and corresponding ribosomal sites in *S. cerevisiae* and *P. locustae*. In microsporidian ribosomes compared with ribosomes from other eukaryotes, the helix H52 is truncated. In *V. necatrix*, the void of the truncated H52 is filled with msL1-*Vn*, and in the *E. cuniculi* ribosomes, this void is filled with msL1-*Ec*. c) A side-by-side comparison of the molecular surroundings of msL1-*Vn*, msL2-*Ec*, and H52 in the ribosome from different species.

Results

The msL1/msL2 Fold Switch in Microsporidian Species

To better understand how the proteins msL1-*Vn* and msL2-*Ec* could have changed their fold during their evolution, we first compared their structures and ribosome attachment mechanisms. Both msL1-*Vn* and msL2-*Ec* were clearly visualized in the cryo-EM structures of their respective ribosomes (PDB accession codes 6RM3 and 7QEP) and display unique and distinct folds compared with each other and with AlphaFold predictions (Barandun et al. 2019; Nicholson et al. 2022; Fig. 1a, supplementary fig. 1, Supplementary Material online).

Although the 2 proteins are of identical length (72 amino acids), share 41% sequence similarity, and also share some secondary structure similarity, namely 2 short α-helical segments (residues 23 to 40 and 58 to 68), the overall folds are very dissimilar with a backbone RMSD value of 11.4 Å.

We next compared the ribosomal binding mode and location of msL1-*Vn* and msL2-*Ec*. While msL1-*Vn* and msL2-*Ec* are attached to the same, although variable in size, 25S rRNA helix H52 in the large ribosomal subunit, our analysis showed that in *V. necatrix* ribosomes, the N-terminus of msL1-*Vn* is directed toward the solvent-exposed side of the ribosome, whereas in *E. cuniculi* ribosomes, the N-terminus of msL2-*Ec* is oriented in the opposite direction, toward the ribosomal core. Thus, the proteins msL1-*Vn* and msL2-*Ec* are inverted relative to each other in the ribosome structure, pointing their N-termini and C-termini in opposite directions (Fig. 1b).

Next, we aimed to understand whether the conserved residues of these proteins make conserved contacts with the ribosome. Given the extent of sequence similarity between msL1-*Vn* and msL2-*Ec* (41% similarity), we compared the molecular contacts of 21 identical and 8 similar residues with the ribosome. We found that most of these conserved residues mediated msL1-*Vn*/msL2-*Ec* attachment to the ribosome; strikingly, however, none of them bound the ribosome in a similar manner in both proteins. For example, in *V. necatrix* ribosomes, the conserved motif ^{43}KIKxLKxKK^{51} of msL1-*Vn* bound the bundle of rRNA helices H5/H8/H10/H52/H53, whereas in *E. cuniculi* ribosomes, the same motif was moved ∼22 Å away, binding a different bundle, H55/H56/H66 (Fig. 1b and c).

Overall, our analysis revealed a vivid contrast between a relatively high conservation of msL1-*Vn*/msL2-*Ec* sequences and a complete change of fold. Thus, msL1-*Vn* and msL2-*Ec* represent a new example of proteins classified as sequence homologs that adopt dissimilar folds and completely repurpose their conserved residues in the ribosome structure to retain their biological function.

Each Microsporidian Lineage Bears a Dissimilar Ortholog of msL1/msL2

To better understand the evolution of msL1/msL2 folds, we next compared msL1-*Vn* and msL2-*Ec* with their structurally uncharacterized homologs from other microsporidian species. In doing so, we sought to understand whether these uncharacterized homologs resemble msL1-*Vn* or msL2-*Ec* in ribosome attachment and possibly in fold. To address this, we first searched for msL1/msL2 homologs in the NCBI genome database using a sensitive homolog search based on hidden Markov models (supplementary materials and methods, Supplementary Material online; supplementary data S1, Supplementary Material online). This search did not detect any msL1/msL2 homologs outside of the microsporidian clade but revealed detectable msL1/msL2 homologs in 16 of the 24 characterized microsporidian species, especially in the microsporidian clades that are most distant from other eukaryotic species and exhibit the highest extent of genome reduction and rRNA reduction (Fig. 2a to c).

We then assessed the sequence similarity between these homologs and msL1-*Vn* and msL2-*Ec* (Fig. 2c; supplementary figs. S1 and S2, Supplementary Material online). We found that among *Encephalitozoon* species, msL1/msL2 homologs shared >95% of sequence conservation in those residues that mediate the ribosome attachment of msL2-*Ec*, suggesting that in *Encephalitozoon* species, these homologs share the same ribosome attachment strategy and possibly the same fold as in msL2-*Ec*. We also found that msL1-*Vn* shared <48% sequence conservation in those residues that mediate ribosome attachment in msL2-*Ec*, consistent with the fact that msL1-*Vn* has a dissimilar ribosome attachment strategy and fold compared with those of msL2-*Ec*.

The most rapidly evolving residues are located in the middle of the msL1/msL2 molecules (residues 38 to 39 in msL1-*Vn*) and at the C-terminus (residues 69 to 73 in msL1-*Vn*). However, despite sequence variability, these segments have the same secondary structure (Fig. 2a). The most conserved residues cluster in 2 segments of msL1/msL2: at the N-terminus, which contains the ^{7}KxKW^{10} motif that is conserved among all msL1/msL2 homologs, and in the loop in the middle of the msL1/msL2 polypeptide chain, which contains the highly conserved ^{47}LKxKK^{51} motif. However, regardless of their conservation, even the most conserved residues in msL1/msL2 have entirely dissimilar surroundings in the ribosome from *E. cuniculi* compared with the ribosome from *V. necatrix* (Fig. 2c).

Remarkably, we found that the remaining microsporidian species carried mutations in most of the residues that are responsible for ribosome attachment of msL1-*Vn* or msL2-*Ec* (Fig. 2a to c). For example, the *Trachipleistophora hominis* homolog of msL1/msL2 carries mutations in ∼66% of the ribosome-binding residues of msL1-*Vn* and 68% of the ribosome-binding residues of msL2-*Ec*. Hence, if the msL1/msL2 homolog from *T. hominis* has the same fold as msL1-*Vn* or msL2-*Ec*, it would carry mutations in most of its ribosome-binding residues. This high variability of the ribosome-binding interface suggests that each lineage of microsporidian parasites (such as *Encephalitozoon*, *Nosematidae*, *Enterospora*, and *Trachipleistophora*) may encode structurally dissimilar variants of msL1/msL2.

The msL1/msL2 Fold Change Is Likely Caused by rRNA Truncation

Finally, to understand what may have caused the fold and orientation switch between msL1-*Vn* and msL2-*Ec*, we compared the molecular surroundings of these proteins in the ribosome. We hypothesized that alterations in ribosomal structure at the binding site may have induced a co-evolutionary adaptation in the msL1/msL2 protein to maintain binding. To test this idea, we first superposed the structures of the *V. necatrix* and *E. cuniculi* ribosomes and found that the msL1/msL2-binding pockets are not identical, with the most prominent difference present in

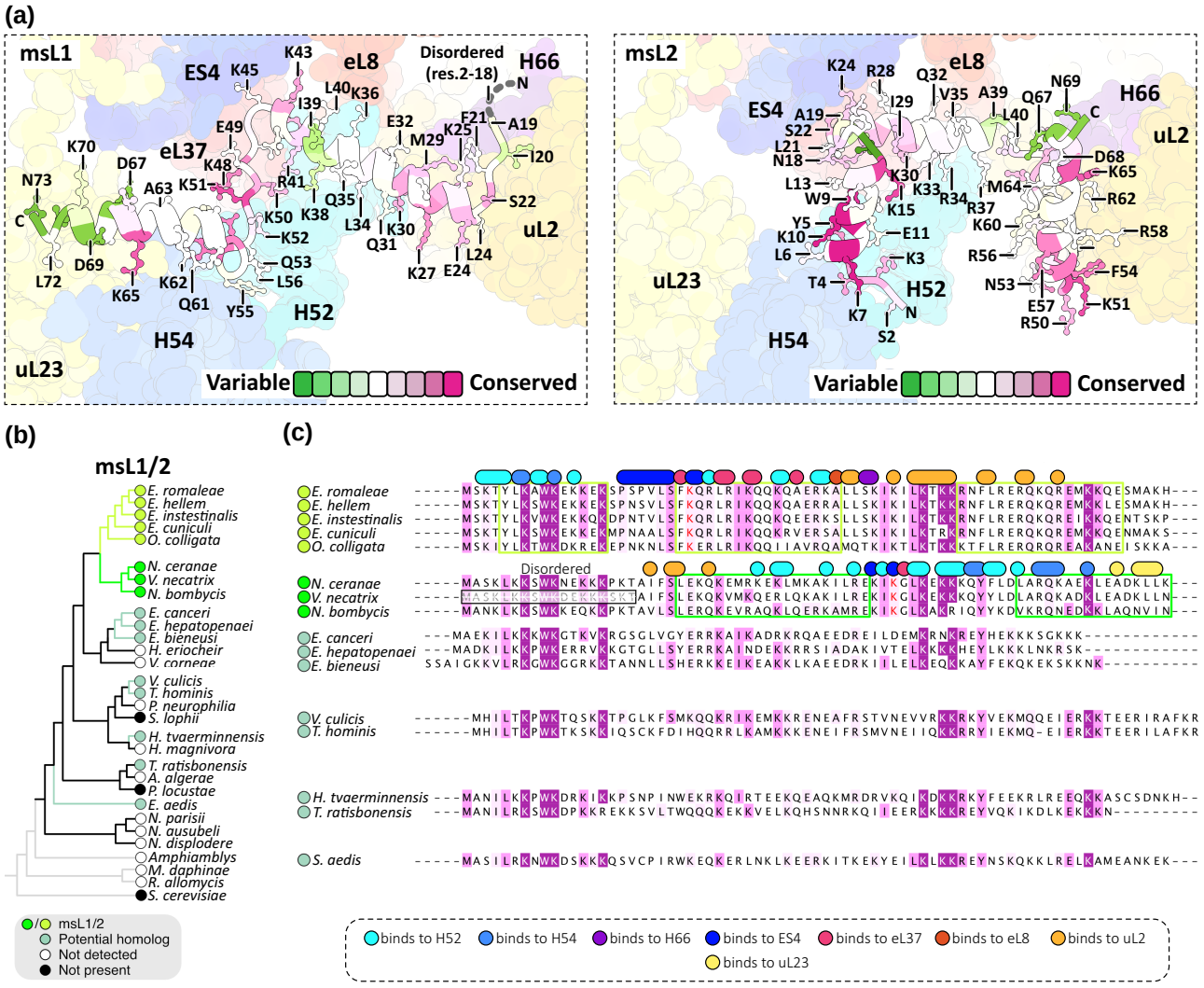

Fig. 2. Each lineage of microsporidians encodes a dissimilar ortholog of msL1/msL2. a) The structures of msL1-*Vn* and msL2-*Ec* are shown in their ribosome-binding sites and colored by the conservation of their residues across microsporidian species. The panel shows that the ribosome-binding residues of msL1-*Vn* and msL2-*Ec* include both highly conserved and highly variable residues and that the highly conserved residues of msL1/msL2 (e.g. K65) have dissimilar locations in the ribosome structure in *V. necatrix* (left panel) compared with *E. cuniculi* (right panel). b) A ribosomal protein-based phylogenetic tree highlights microsporidian species with detectable msL1/msL2 homologs. The label "not detected" indicates that the absence of msL1/msL2 homologs in corresponding microsporidian species was inferred from sequence-based homology searches. The label "not present" indicates that the molecular structure of ribosomes from the corresponding microsporidian species was determined and showed the absence of msL1/msL2 homologs in the ribosome. c) A multiple sequence alignment illustrates the conservation of msL1/msL2 homologs from different microsporidian species. This alignment also highlights residues in msL1-*Vn* and msL2-*Ec* that are involved in ribosome binding. Each of these ribosome-binding residues is indicated as a circle or an oval above the aligned sequences and is colored by their molecular partner in the ribosome structure. The boxes around aligned sequences indicate the helical segments of msL1-*Vn* and msL2-*Ec*.

helix H52 of the 25S rRNA (Fig. 3a). This helix is 3 bases shorter in *E. cuniculi* compared with the *V. necatrix* ribosome. Strikingly, if the *V. necatrix* helix were the same size as in *E. cuniculi*, it would occlude 24% of the ribosome-binding surface for msL1-*Vn*, potentially explaining why msL1-*Vn*/msL2-*Ec* cannot adopt the same fold in the *E. cuniculi* and *V. necatrix* ribosomes.

Because this finding suggested that the H52 truncation was a major driver of the msL1-*Vn*/msL2-*Ec* fold switch, we next assessed the length of H52 across microsporidian species (Fig. 3a; supplementary data S2, Supplementary Material online). We found that in typical eukaryotes, such as *Saccharomyces cerevisiae* and humans, H52 comprises ~60 rRNA bases, whereas in microsporidian species, H52 is reduced to 12 to 33 bases. We observe msL1/msL2 orthologs in every sequenced microsporidian lineage with short H52s (12 to 18 bases) but a more sporadic presence of msL1/msL2 in lineages with longer H52s (19 to 24 bases). *Paranosema locustae*, in which we did not detect an msL1/msL2 homolog, has a longer H52 (20 bases), and the previously published structure of its ribosome (PDB accession code 6ZU5) confirms the absence of msL1/msL2 (Ehrenbolger et al. 2020). Docking msL1-*Vn* and msL2-*Ec* into their ribosomal binding sites on the *P. locustae* or *S. cerevisiae* ribosome revealed that the longer H52 would not be able to accommodate msL1-*Vn* nor msL2-*Ec* (Fig. 3b).

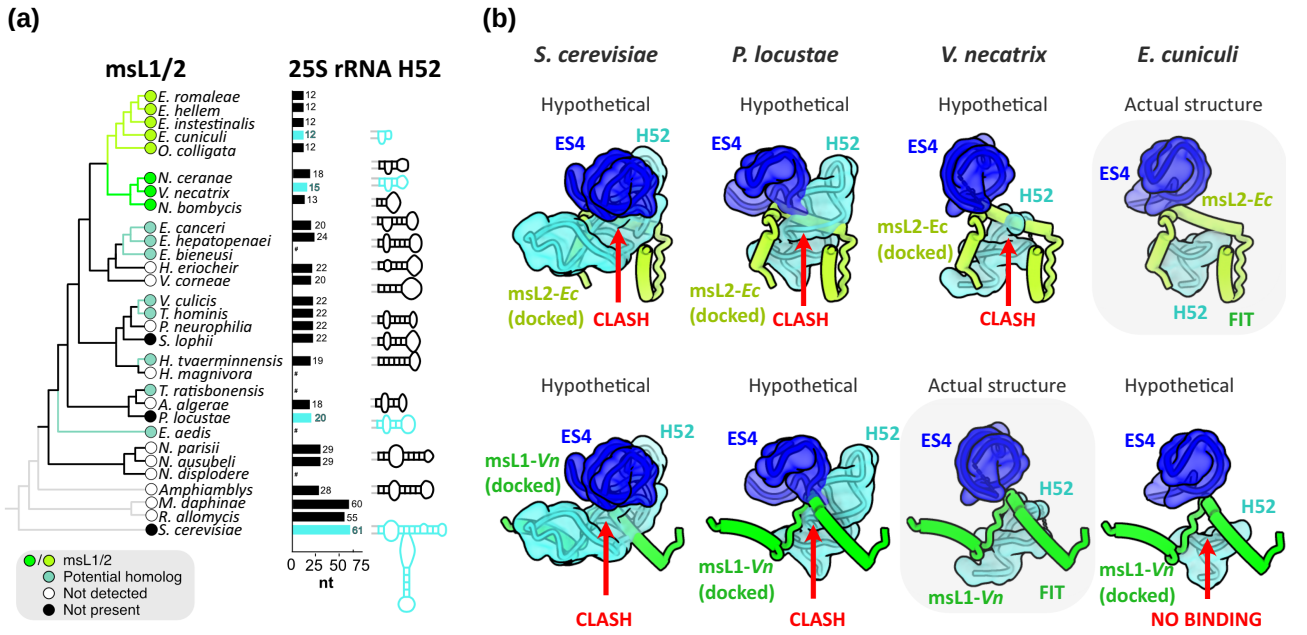

Fig. 3. The msL1/msL2 fold change is likely caused by rRNA truncations. a) A ribosomal protein–based phylogenetic tree is shown with detectable msL1/msL2 homologs indicated. For species with available 5.8S-25S rRNA sequences, the length and predicted secondary structure of the helix H52 are shown next to their corresponding species. Species with missing or incomplete sequences for 5.8S-25S rRNA are highlighted by asterisks, and species with experimentally defined ribosome structures are highlighted in cyan. The label "not detected" indicates that the absence of msL1/msL2 homologs in corresponding microsporidian species was inferred from sequence-based homology searches. The label "not present" indicates that the molecular structure of ribosomes from the corresponding microsporidian species was determined and showed the absence of msL1/msL2 homologs in the ribosome. b) The structures of msL1-*Vn* and msL2-*Ec* docked into the ribosomal environment of the *S. cerevisiae*, *P. locustae*, *V. necatrix*, and *E. cuniculi* ribosomes to illustrate potential steric clashes or loss of ribosome-binding surface in one species relative to each other. Each docking was performed by superimposing ribosome structures from the *E. cuniculi* and *V. necatrix* with ribosome structures with other eukaryotic species.

Collectively, our findings suggest that variations in rRNA size can indeed be a driver of the msL1-*Vn*/msL2-*Ec* fold change.

Discussion

A Conserved Ribosomal Protein Has Entirely Dissimilar Folds in Different Organisms

In this study, we capitalized on the recent advances in structural studies of microsporidian ribosomes to explore how ribosomes alter new ribosomal proteins during their evolution. This approach enabled us to identify an evolutionary fold switch in the ribosomal protein msL1/msL2, which would be impossible to observe using computational predictions or sequence analyses. We found that this ribosomal protein underwent a nearly complete transformation of its secondary and 3D structure, while retaining its ability to recognize the same specific ribosomal helix, H52, in one organism compared with another.

This finding has several implications for our understanding of how large macromolecular machines, including ribosomes, acquire new subunits and influence their structural fold across evolutionary time. First, our work allows us to reevaluate the concept of structural mimics: structurally dissimilar proteins that occupy the same site in a given macromolecular complex from different species (Harms et al. 2001). For example, in bacterial ribosomes, protein bL34 occupies the same site as protein eL37 in eukaryotic ribosomes (Harms et al. 2001). Because bL34 is composed of β-sheets and eL37 of α-helices and these proteins share only 19% of sequence similarity, they are assumed to have independent evolutionary origins. However, the example of msL1/msL2 (although these proteins have twice higher sequence similarity) highlights that a lack of structural similarity does not necessarily imply an independent or even distant evolutionary origin (Harms et al. 2001; Klein et al. 2004; Ban et al. 2014).

Also, our study of the msL1/msL2 protein family provides an example where the most conserved protein property may not be its sequence or structure but its position within the macromolecular assembly to which it belongs. Consequently, it is possible that for proteins acting as part of complex molecular assemblies, their position within these assemblies can serve as an additional potential indicator of their evolutionary origin.

It is important to note that, without additional experimental support, our understanding of msL1/msL2 evolution is hypothetical and does not exclude alternative evolutionary scenarios. One such scenario could involve an ancient gene duplication event of the msL1/msL2 predecessor, followed by the specialization of 2 paralogs and the loss of one of these isoforms in certain microsporidian species. The presence or absence of msL1-coding or msL2-coding genes in certain microsporidian clades

could also result from horizontal gene transfer events, among other scenarios. Therefore, it will be important to explore ribosomes from other microsporidian lineages, including those from *Enterocytozoon* and *Vavraia*/*Trachipleistophora*, to better distinguish between these alternative scenarios of msL1/msL2 evolution.

msL1/2 is an Example of an Evolved Fold Switching Without a Loss of Biological Specificity

Previously, the ability of proteins to completely transform their structural fold through evolution has been studied in detail for more than a dozen proteins and was termed as "macrotransitions," "evolutionary metamorphosis," or "evolved fold switching" (Grishin 2001; Alva et al. 2008; Alexander et al. 2009; Farias-Rico et al. 2014; Andreeva et al. 2015; Toledo-Patino et al. 2019; Kolodny et al. 2021; Chakravarty et al. 2023). One of the most striking examples of this metamorphosis was found in *Streptococcus* protein G, where the substitution of just a single amino acid, L45Y, alters 85% of the protein's secondary structure, transforming the serum-binding domain protein G_A into the immunoglobulin G-binding domain protein G_B (Alexander et al. 2009). In these previously studied examples, however, the observed fold change was typically accompanied by a change in the biological function of a given protein. In contrast, we showed that protein msL1/msL2 changes its fold while retaining its ability to recognize one specific partner: of all possible binding sites in a cell, this protein retains its ability to bind a specific site of the ribosome at the tip of 25S rRNA helix H52. This example shows that a protein can, in the right context, undergo evolved fold switching without function loss.

msL1/2 is an Example of Fold Switching Likely Driven by Changes in Its Binding Partner

Recent advances in protein structural prediction by AlphaFold2, Evolutionary Scale Modeling, and other artificial intelligence-based tools have shifted the gravity of protein studies toward Anfinsen's folders, globular proteins whose structures are determined by their amino acid sequences (Xu and Zhang 2013; Ovchinnikov et al. 2017; Deng et al. 2019; Sillitoe et al. 2019; Andreeva et al. 2020; Gligorijevic et al. 2021; Jumper et al. 2021; Pereira et al. 2021; Aderinwale et al. 2022). Nature, however, carries a high number of protein families that either require chaperones to fold into a certain structure or that lack globular domains altogether and remain intrinsically disordered unless they bind to other molecules (Oldfield and Dunker 2014; Uversky 2016; Pancsa et al. 2018; Macossay-Castillo et al. 2019). Based on recent estimates, these nonglobular and intrinsically disordered proteins include >1,150 protein families, and >50% of eukaryotic proteins were shown to bear at least one long disordered segment (Tompa 2012; Wright and Dyson 2015; Contreras-Martos et al. 2018; Kulkarni and Uversky 2018; Toto et al. 2022). This abundance of nonglobular proteins, along with their frequent omission from structural studies, raises the question: do they follow the same principle of evolutionary fold switching as their globular counterparts?

Our analysis of msL1/msL2 protein provides one possible answer to this question: msL1/msL2 is a typical nonglobular protein in both *E. cuniculi* and *V. necatrix*, and our computational analysis revealed that the sequences of all known msL1/msL2 homologs are characterized by high levels of predicted intrinsic disorder (see supplementary figs. S2 and S3, Supplementary Material online). The fact that the structures of msL1 and msL2 are similar when predicted by Alphafold but differ from the experimentally determined ribosome-bound structures indicates that the ribosome-bound structures of msL1/msL2 are likely defined by their contacts with the ribosome. Specifically, the rRNA helix H52 appears to promote the folding of msL1/msL2 by neutralizing the positive charge of the msL1/msL2 molecule.

Overall, our analysis suggests an evolutionary scenario in which ancient microsporidians have lost one of their rRNA segments (ES31L) and evolved a new protein through de novo gene birth to counteract the negative impact of the rRNA truncation. As microsporidians continued to undergo degeneration of their rRNA, the new ribosomal protein underwent a fold switch to maintain its binding to the ribosome despite structural changes in how it engages with the ribosome. This scenario can be depicted by a classical Sewall Wright adaptive fitness landscape, where deleterious mutations in rRNA are compensated by the emergence and subsequent evolution of a novel ribosomal protein (Fig. 4). This model is consistent with previous work demonstrating that microsporidian rRNA appears to evolve faster than their ribosomal proteins (Peyretaillade et al. 1998; Lecompte et al. 2002; O'Mahony et al. 2007; Melnikov et al. 2018a, 2018b; Barandun et al. 2019; Ehrenbolger et al. 2020; Wadi and Reinke 2020; Jespersen et al. 2022; Nicholson et al. 2022). Thus, our study of msL1/msL2 provides strong evidence that, in nonglobular proteins, evolutionary changes in their binding partners can serve as the major driver of an evolutionary fold switch.

Materials and Methods

Comparative Analysis of Microsporidian Ribosome Structures

The msL1/msL2 structures in the *E. cuniculi* and *V. necatrix* ribosomes were compared using Coot (0.9.4.1) to superpose structures, measure intermolecular and intramolecular distances, and calculate the RMSD between protein backbone residues (Emsley et al. 2010). The contact area between msL1/msL2 and rRNA was calculated using the CCP4 package AreaIMol 8.0.001, with the solvent sphere diameter set to 1.7 Å (Hough and Wilson 2018). The figures were prepared using ChimeraX 1.2.5 (Pettersen et al. 2021). Intrinsic disorder propensities of the ribosomal proteins from the msL1/msL2 family were evaluated by the PONDR VLXT computational tool (Romero et al. 2001). To evaluate global disorder predisposition of a query protein, we calculated the percent of predicted disordered residues (i.e. residues with disorder scores above 0.5) and

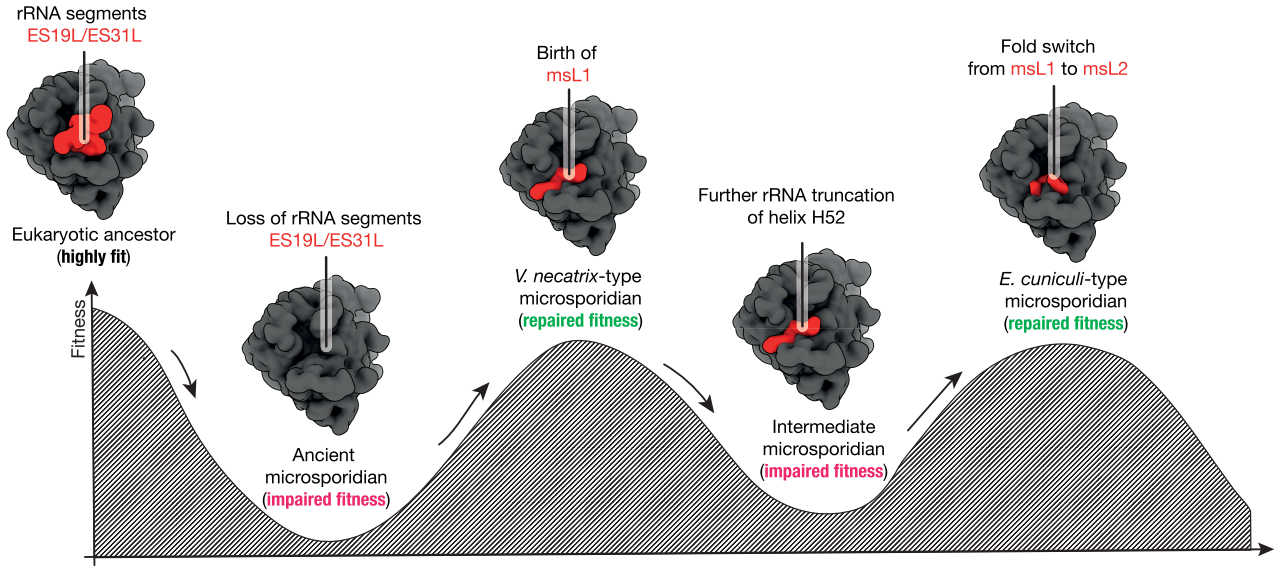

Fig. 4. A hypothetical evolutionary scenario of the origin and fold switch of ribosomal protein msL1/msL2. The Sewall Wright's adaptive fitness landscape shows a possible order of events in which the degeneration of rRNA in microsporidian species was compensated by the origin and subsequent evolution of a new ribosomal protein. In this hypothetical order of events, microsporidian species have undergone a progressive reduction of their ribosomal RNA, which was likely caused by the accumulation of deleterious mutations in microsporidian genomes due to frequent genetic drifts. Then, a new protein msL1 could originate through the spontaneous de novo birth of a gene that was retained in microsporidia due to its ability to counterbalance the rRNA reduction. As rRNA continued to evolve and reduce in size, protein msL1 then underwent a fold switch to yield protein msL2 with improved affinity to its ribosomal binding site (i.e. truncated helix H52).

calculated the average disorder score as a protein length–normalized sum of all the per-residue disorder scores in a query protein. For further classification of these proteins, we used a Charge-Hydropathy versus Cummulative-Distribution-Function analysis (CH-CDF) (Mohan et al. 2008; Huang et al. 2012, 2014).

Structure Prediction Using AlphaFold

Structural model predictions were carried out using the AlphaFold Colab Notebook (version 2.3.2; Mirdita 2022) using the full sequences of msL1-*Vn* and msL2-*Ec*. All modeling was performed using default parameters without any additional environmental factors, and the structures were visualized in ChimeraX 1.2.5 (Pettersen et al. 2021).

Searching for msL1/msL2 Homologs

Putative msL1/msL2 homologs were identified using 2 iterations of HMMER (Finn et al. 2011), with sequences of msL1/msL2 from either *E. cuniculi* or *V. necatrix* as the initial input. For each search iteration, we used the following search options: -E 1 --domE 1 --incE 0.01 --incdomE 0.03 --seqdb uniprotrefprot. To maximize the success rate, the search was repeated using the following databases of protein sequences: Reference Proteomes, UniProtKB, Swiss-Prot, and Ensemble. The obtained results from each of these searches were combined, reduced to remove redundant findings, and listed (supplementary data S1, Supplementary Material online). The identified sequences of msL1, msL2, and their apparent homologs were then used as an input file to assess the conservation of msL1/msL2 residues using Rate4Site 2.01 with the default parameters (Pupko 2002).

Analysis of Variations in Microsporidian rRNA

Due to the anomalously short length of rRNA from microsporidian species compared with other eukaryotes, many microsporidian rRNA sequences are typically excluded from such commonly used databases of rRNA sequences such as SILVA due to its "truncated sequences" filter (Quast et al. 2013). Therefore, to analyze variations in microsporidian rRNA, microsporidian 25S rRNA sequences were consolidated using the SILVA ribosomal RNA gene database (Quast et al. 2013), the RNAcentral database (The RNAcentral Consortium 2019), MicrosporidiaDB (Warrenfeltz et al. 2018), as well as local genome databases for *V. necatrix* and *P. locustae*. These sequences were then aligned using Clustal Omega with default parameters, the resulting alignment is shown in (supplementary data S2, Supplementary Material online). Where available, ribosomal structures were used to manually model the 2D structures of helix H52. These structures included the models of *S. cerevisiae* (PDB 4V88), *V. necatrix* (PDB 6RM3), *P. locustae* (PDB 6ZU5), and *E. cuniculi* (PDB 7QEP) ribosomes. For the remaining species, respective segments of the 25S rRNA alignment were used to predict 2D structures with Mfold using the RNA Folding Form feature (Zuker 2003). The sequences corresponding to the 2D structures of Helix H52 were then assessed to calculate the total length of the rRNA segment in each microsporidian species.

Assembling a Microsporidian Phylogenetic Tree

The microsporidian phylogeny shown in (Figs. 2b and 3a) was assembled using sequences of all microsporidian ribosomal protein. Protein sequences for *V. necatrix* and *P. locustae* were procured from local databases (Barandun et al.

2019; Ehrenbolger et al. 2020). Ribosomal protein sequences were retrieved by using the translated nucleotide blast (tblastn) with an E-value cutoff of 0.05 based on the sequences of the *S. cerevisiae* or *V. necatrix* hits as query and the NCBI NIH and the MicrosporidiaDB (Warrenfeltz et al. 2018) as the search databases. The protein sequences were aligned using MUSCLE (Edgar 2004), followed by trimming with trimAl (Capella-Gutierrez et al. 2009) using the "–gappyout" option. Trimmed alignments were subsequently concatenated using FASconCAT (Kuck and Meusemann 2010). The resulting phylogenetic tree was assembled with IQ-TREE and visualized using FigTree.v1.4.4 and employing *S. cerevisiae* as the root.

Supplementary Material

Supplementary material is available at *Molecular Biology and Evolution* online.

Acknowledgments

We thank the personnel in the Barandun and Melnikov laboratories for their help with the manuscript preparation and Johan Panek (Newcastle University, UK) for his critical comments.

Funding

This work was funded by the Biotechnology and Biological Sciences Research Council BB/T008695/1 (to C.R.B.), the Newcastle University Oversears Research Scholarship 2021 award (to K.H-B.), the Swedish Research Council (2019-02011), the H2020 European Research Council (ERC Starting Grant PolTube 948655), the Science for Life Laboratory National Fellows program, and The Laboratory for Molecular Infection Medicine Sweden (all to J.B.) and the Horizon 2020 Framework programme (the Grant Agreement No. 895166 to S.V.M.).

References

Aderinwale T, Bharadwaj V, Christoffer C, Terashi G, Zhang Z, Jahandideh R, Kagaya Y, Kihara D. Real-time structure search and structure classification for AlphaFold protein models. *Commun Biol*. 2022:**5**(1):316. https://doi.org/10.1038/s42003-022-03261-8.

Alexander PA, He Y, Chen Y, Orban J, Bryan PN. A minimal sequence code for switching protein structure and function. *Proc Natl Acad Sci U S A*. 2009:**106**(50):21149–21154. https://doi.org/10.1073/pnas.0906408106.

Alva V, Koretke KK, Coles M, Lupas AN. Cradle-loop barrels and the concept of metafolds in protein classification by natural descent. *Curr Opin Struct Biol*. 2008:**18**(3):358–365. https://doi.org/10.1016/j.sbi.2008.02.006.

Alvarez-Carreno C, Gupta RJ, Petrov AS, Williams LD. Creative destruction: new protein folds from old. *Proc Natl Acad Sci U S A*. 2022:**119**(52):e2207897119. https://doi.org/10.1073/pnas.2207897119.

Alvarez-Carreno C, Penev PI, Petrov AS, Williams LD. Fold evolution before LUCA: common ancestry of SH3 domains and OB domains. *Mol Biol Evol*. 2021:**38**(11):5134–5143. https://doi.org/10.1093/molbev/msab240.

Andreeva A, Howorth D, Chothia C, Kulesha E, Murzin AG. Investigating protein structure and evolution with SCOP2. *Curr Protoc Bioinformatics*. 2015:**49**(1):1.26.21–21.26.21. https://doi.org/10.1002/0471250953.bi0126s49.

Andreeva A, Kulesha E, Gough J, Murzin AG. The SCOP database in 2020: expanded classification of representative family and superfamily domains of known protein structures. *Nucleic Acids Res*. 2020:**48**(D1):D376–D382. https://doi.org/10.1093/nar/gkz1064.

Ban N, Beckmann R, Cate JH, Dinman JD, Dragon F, Ellis SR, Lafontaine DL, Lindahl L, Liljas A, Lipton JM, *et al*. A new system for naming ribosomal proteins. *Curr Opin Struct Biol*. 2014:**24**:165–169. https://doi.org/10.1016/j.sbi.2014.01.002.

Barandun J, Hunziker M, Vossbrinck CR, Klinge S. Evolutionary compaction and adaptation visualized by the structure of the dormant microsporidian ribosome. *Nat Microbiol*. 2019:**4**(11):1798–1804. https://doi.org/10.1038/s41564-019-0514-6.

Belousoff MJ, Davidovich C, Zimmerman E, Caspi Y, Wekselman I, Rozenszajn L, Shapira T, Sade-Falk O, Taha L, Bashan A, *et al*. Ancient machinery embedded in the contemporary ribosome. *Biochem Soc Trans*. 2010:**38**(2):422–427. https://doi.org/10.1042/BST0380422.

Bokov K, Steinberg SV. A hierarchical model for evolution of 23S ribosomal RNA. *Nature*. 2009:**457**(7232):977–980. https://doi.org/10.1038/nature07749.

Bose T, Fridkin G, Davidovich C, Krupkin M, Dinger N, Falkovich AH, Peleg Y, Agmon I, Bashan A, Yonath A. Origin of life: protoribosome forms peptide bonds and links RNA and protein dominated worlds. *Nucleic Acids Res*. 2022:**50**(4):1815–1828. https://doi.org/10.1093/nar/gkac052.

Bowman JC, Petrov AS, Frenkel-Pinter M, Penev PI, Williams LD. Root of the tree: the significance, evolution, and origins of the ribosome. *Chem Rev*. 2020:**120**(11):4848–4878. https://doi.org/10.1021/acs.chemrev.9b00742.

Capella-Gutierrez S, Silla-Martinez JM, Gabaldon T. trimAl: a tool for automated alignment trimming in large-scale phylogenetic analyses. *Bioinformatics*. 2009:**25**(15):1972–1973. https://doi.org/10.1093/bioinformatics/btp348.

Chakravarty D, Schafer JW, Porter LL. Distinguishing features of fold-switching proteins. *Protein Sci*. 2023:**32**(3):e4596. https://doi.org/10.1002/pro.4596.

Contreras-Martos S, Nguyen HH, Nguyen PN, Hristozova N, Macossay-Castillo M, Kovacs D, Bekesi A, Oemig JS, Maes D, Pauwels K, *et al*. Quantification of intrinsically disordered proteins: a problem not fully appreciated. *Front Mol Biosci*. 2018:**5**:83. https://doi.org/10.3389/fmolb.2018.00083.

Deng L, Zhong G, Liu C, Luo J, Liu H. MADOKA: an ultra-fast approach for large-scale protein structure similarity searching. *BMC Bioinformatics*. 2019:**20**(S19):662. https://doi.org/10.1186/s12859-019-3235-1.

Di Giulio M. The universal ancestor was a thermophile or a hyperthermophile: tests and further evidence. *J Theor Biol*. 2003:**221**(3):425–436. https://doi.org/10.1006/jtbi.2003.3197.

Edgar RC. MUSCLE: multiple sequence alignment with high accuracy and high throughput. *Nucleic Acids Res*. 2004:**32**(5):1792–1797. https://doi.org/10.1093/nar/gkh340.

Ehrenbolger K, Jespersen N, Sharma H, Sokolova YY, Tokarev YS, Vossbrinck CR, Barandun J. Differences in structure and hibernation mechanism highlight diversification of the microsporidian ribosome. *PLoS Biol*. 2020:**18**(10):e3000958. https://doi.org/10.1371/journal.pbio.3000958.

Emsley P, Lohkamp B, Scott WG, Cowtan K. Features and development of Coot. *Acta Crystallogr D Biol Crystallogr*. 2010:**66**(4):486–501. https://doi.org/10.1107/S0907444910007493.

Farias-Rico JA, Schmidt S, Hocker B. Evolutionary relationship of two ancient protein superfolds. *Nat Chem Biol*. 2014:**10**(9):710–715. https://doi.org/10.1038/nchembio.1579.

Finn RD, Clements J, Eddy SR. HMMER web server: interactive sequence similarity searching. *Nucleic Acids Res*. 2011:**39**(Web Server issue):W29–W37. https://doi.org/10.1093/nar/gkr367.

Fox GE. Origin and evolution of the ribosome. *Cold Spring Harb Perspect Biol*. 2010:**2**(9):a003483. https://doi.org/10.1101/cshperspect.a003483.

Fox GE, Tran Q, Yonath A. An exit cavity was crucial to the polymerase activity of the early ribosome. *Astrobiology*. 2012:**12**(1):57–60. https://doi.org/10.1089/ast.2011.0692.

Gligorijevic V, Renfrew PD, Kosciolek T, Leman JK, Berenberg D, Vatanen T, Chandler C, Taylor BC, Fisk IM, Vlamakis H, *et al*. Structure-based protein function prediction using graph convolutional networks. *Nat Commun*. 2021:**12**(1):3168. https://doi.org/10.1038/s41467-021-23303-9.

Grishin NV. Fold change in evolution of protein structures. *J Struct Biol*. 2001:**134**(2-3):167–185. https://doi.org/10.1006/jsbi.2001.4335.

Harms J, Schluenzen F, Zarivach R, Bashan A, Gat S, Agmon I, Bartels H, Franceschi F, Yonath A. High resolution structure of the large ribosomal subunit from a mesophilic eubacterium. *Cell*. 2001:**107**(5):679–688. https://doi.org/10.1016/S0092-8674(01)00546-3.

Hough MA, Wilson KS. From crystal to structure with CCP4. *Acta Crystallogr D Struct Biol*. 2018:**74**(2):67. https://doi.org/10.1107/S2059798317017557.

Hu EZ, Lan XR, Liu ZL, Gao J, Niu DK. A positive correlation between GC content and growth temperature in prokaryotes. *BMC Genomics*. 2022:**23**(1):110. https://doi.org/10.1186/s12864-022-08353-7.

Hu XP, Lercher MJ. An optimal growth law for RNA composition and its partial implementation through ribosomal and tRNA gene locations in bacterial genomes. *PLoS Genet*. 2021:**17**(11):e1009939. https://doi.org/10.1371/journal.pgen.1009939.

Huang F, Oldfield C, Meng J, Hsu WL, Xue B, Uversky VN, Romero P, Dunker AK. Subclassifying disordered proteins by the CH-CDF plot method. *Pac Symp Biocomput*. 2012:128–139. https://doi.org/10.1142/9789814366496_0013.

Huang F, Oldfield CJ, Xue B, Hsu WL, Meng J, Liu X, Shen L, Romero P, Uversky VN, Dunker A. Improving protein order-disorder classification using charge-hydropathy plots. *BMC Bioinformatics*. 2014:**15**(Suppl 17):S4. https://doi.org/10.1186/1471-2105-15-S17-S4.

Jespersen N, Monrroy L, Barandun J. Impact of genome reduction in microsporidia. In: Weiss LM, Reinke AW, editors. *Microsporidia. Experientia supplementum*. Vol. 114. Cham: Springer; 2022. p. 1–42.

Jumper J, Evans R, Pritzel A, Green T, Figurnov M, Ronneberger O, Tunyasuvunakool K, Bates R, Zidek A, Potapenko A, *et al*. Highly accurate protein structure prediction with AlphaFold. *Nature*. 2021:**596**(7873):583–589. https://doi.org/10.1038/s41586-021-03819-2.

Khachane AN, Timmis KN, dos Santos VA. Uracil content of 16S rRNA of thermophilic and psychrophilic prokaryotes correlates inversely with their optimal growth temperatures. *Nucleic Acids Res*. 2005:**33**(13):4016–4022. https://doi.org/10.1093/nar/gki714.

Kimura H, Ishibashi J, Masuda H, Kato K, Hanada S. Selective phylogenetic analysis targeting 16S rRNA genes of hyperthermophilic archaea in the deep-subsurface hot biosphere. *Appl Environ Microbiol*. 2007:**73**(7):2110–2117. https://doi.org/10.1128/AEM.02800-06.

Kimura H, Mori K, Yamanaka T, Ishibashi J. Growth temperatures of archaeal communities can be estimated from the guanine-plus-cytosine contents of 16S rRNA gene fragments. *Environ Microbiol Rep*. 2013:**5**(3):468–474. https://doi.org/10.1111/1758-2229.12035.

Klein DJ, Moore PB, Steitz TA. The roles of ribosomal proteins in the structure assembly, and evolution of the large ribosomal subunit. *J Mol Biol*. 2004:**340**(1):141–177. https://doi.org/10.1016/j.jmb.2004.03.076.

Kolodny R, Nepomnyachiy S, Tawfik DS, Ben-Tal N. Bridging themes: short protein segments found in different architectures. *Mol Biol Evol*. 2021:**38**(6):2191–2208. https://doi.org/10.1093/molbev/msab017.

Kovacs NA, Petrov AS, Lanier KA, Williams LD. Frozen in time: the history of proteins. *Mol Biol Evol*. 2017:**34**(5):1252–1260. https://doi.org/10.1093/molbev/msx086.

Kuck P, Meusemann K. FASconCAT: convenient handling of data matrices. *Mol Phylogenet Evol*. 2010:**56**(3):1115–1118. https://doi.org/10.1016/j.ympev.2010.04.024.

Kulkarni P, Uversky VN. Intrinsically disordered proteins: the dark horse of the dark proteome. *Proteomics*. 2018:**18**(21-22):e1800061. https://doi.org/10.1002/pmic.201800061.

Lecompte O, Ripp R, Thierry JC, Moras D, Poch O. Comparative analysis of ribosomal proteins in complete genomes: an example of reductive evolution at the domain scale. *Nucleic Acids Res*. 2002:**30**(24):5382–5390. https://doi.org/10.1093/nar/gkf693.

Macossay-Castillo M, Marvelli G, Guharoy M, Jain A, Kihara D, Tompa P, Wodak SJ. The balancing act of intrinsically disordered proteins: enabling functional diversity while minimizing promiscuity. *J Mol Biol*. 2019:**431**(8):1650–1670. https://doi.org/10.1016/j.jmb.2019.03.008.

Melnikov S, Ben-Shem A, Garreau de Loubresse N, Jenner L, Yusupova G, Yusupov M. One core, two shells: bacterial and eukaryotic ribosomes. *Nat Struct Mol Biol*. 2012:**19**(6):560–567. https://doi.org/10.1038/nsmb.2313.

Melnikov S, Ben-Shem A, Yusupova G, Yusupov M. Insights into the origin of the nuclear localization signals in conserved ribosomal proteins. *Nat Commun*. 2015:**6**(1):7382. https://doi.org/10.1038/ncomms8382.

Melnikov SV, Khabibullina NF, Mairhofer E, Vargas-Rodriguez O, Reynolds NM, Micura R, Soll D, Polikanov YS. Mechanistic insights into the slow peptide bond formation with D-amino acids in the ribosomal active site. *Nucleic Acids Res*. 2019:**47**(4):2089–2100. https://doi.org/10.1093/nar/gky1211.

Melnikov S, Kwok HS, Manakongtreecheep K, van den Elzen A, Thoreen CC, Soll D. Archaeal ribosomal proteins possess nuclear localization signal-type motifs: implications for the origin of the cell nucleus. *Mol Biol Evol*. 2020:**37**(1):124–133. https://doi.org/10.1093/molbev/msz207.

Melnikov SV, Manakongtreecheep K, Rivera KD, Makarenko A, Pappin DJ, Soll D. Muller's ratchet and ribosome degeneration in the obligate intracellular parasites microsporidia. *Int J Mol Sci*. 2018b:**19**(12):4125. https://doi.org/10.3390/ijms19124125.

Melnikov S, Manakongtreecheep K, Soll D. Revising the structural diversity of ribosomal proteins across the three domains of life. *Mol Biol Evol*. 2018a:**35**(7):1588–1598. https://doi.org/10.1093/molbev/msy021.

Mirdita M, Schütze K, Moriwaki Y, Heo L, Ovchinnikov S, Steinegger M. ColabFold: making protein folding accessible to all. *Nat Methods*. 2022:**19**(6):679–682. https://doi.org/10.1038/s41592-022-01488-1.

Mohan A, Sullivan WJ Jr, Radivojac P, Dunker AK, Uversky VN. Intrinsic disorder in pathogenic and non-pathogenic microbes: discovering and analyzing the unfoldomes of early-branching eukaryotes. *Mol Biosyst*. 2008:**4**(4):328–340. https://doi.org/10.1039/b719168e.

Nicholson D, Salamina M, Panek J, Helena-Bueno K, Brown CR, Hirt RP, Ranson NA, Melnikov SV. Adaptation to genome decay in the structure of the smallest eukaryotic ribosome. *Nat Commun*. 2022:**13**(1):591. https://doi.org/10.1038/s41467-022-28281-0.

Oldfield CJ, Dunker AK. Intrinsically disordered proteins and intrinsically disordered protein regions. *Annu Rev Biochem*. 2014:**83**(1):553–584. https://doi.org/10.1146/annurev-biochem-072711-164947.

O'Mahony EM, Tay WT, Paxton RJ. Multiple rRNA variants in a single spore of the microsporidian *Nosema bombi*. *J Eukaryot Microbiol*.

2007:**54**(1):103–109. https://doi.org/10.1111/j.1550-7408.2006.00232.x.

Ovchinnikov S, Park H, Varghese N, Huang PS, Pavlopoulos GA, Kim DE, Kamisetty H, Kyrpides NC, Baker D. Protein structure determination using metagenome sequence data. *Science*. 2017:**355**(6322):294–298. https://doi.org/10.1126/science.aah4043.

Pancsa R, Zsolyomi F, Tompa P. Co-evolution of intrinsically disordered proteins with folded partners witnessed by evolutionary couplings. *Int J Mol Sci*. 2018:**19**(11):3315. https://doi.org/10.3390/ijms19113315.

Pereira J, Simpkin AJ, Hartmann MD, Rigden DJ, Keegan RM, Lupas AN. High-accuracy protein structure prediction in CASP14. *Proteins*. 2021:**89**(12):1687–1699. https://doi.org/10.1002/prot.26171.

Petrov AS, Bernier CR, Hsiao C, Norris AM, Kovacs NA, Waterbury CC, Stepanov VG, Harvey SC, Fox GE, Wartell RM, *et al*. Evolution of the ribosome at atomic resolution. *Proc Natl Acad Sci U S A*. 2014:**111**(28):10251–10256. https://doi.org/10.1073/pnas.1407205111.

Petrov AS, Gulen B, Norris AM, Kovacs NA, Bernier CR, Lanier KA, Fox GE, Harvey SC, Wartell RM, Hud NV, *et al*. History of the ribosome and the origin of translation. *Proc Natl Acad Sci U S A*. 2015:**112**(50):15396–15401. https://doi.org/10.1073/pnas.1509761112.

Pettersen EF, Goddard TD, Huang CC, Meng EC, Couch GS, Croll TI, Morris JH, Ferrin TE. UCSF ChimeraX: structure visualization for researchers, educators, and developers. *Protein Sci*. 2021:**30**(1):70–82. https://doi.org/10.1002/pro.3943.

Peyretaillade E, Biderre C, Peyret P, Duffieux F, Metenier G, Gouy M, Michot B, Vivares CP. Microsporidian *Encephalitozoon cuniculi*, a unicellular eukaryote with an unusual chromosomal dispersion of ribosomal genes and a LSU rRNA reduced to the universal core. *Nucleic Acids Res*. 1998:**26**(15):3513–3520. https://doi.org/10.1093/nar/26.15.3513.

Polikanov YS, Melnikov SV, Söll D, Steitz TA. Structural insights into the role of rRNA modifications in protein synthesis and ribosome assembly. *Nat Struct Mol Biol*. 2015:**22**(4):342–344. https://doi.org/10.1038/nsmb.2992.

Pupko T, Bell RE, Mayrose I, Glaser F, Ben-Tal N. Rate4Site: an algorithmic tool for the identification of functional regions in proteins by surface mapping of evolutionary determinants within their homologues. *Bioinformatics*. 2002:**18 Suppl 1**:S71–S77. https://doi.org/10.1093/bioinformatics/18.suppl_1.S71.

Quast C, Pruesse E, Yilmaz P, Gerken J, Schweer T, Yarza P, Peplies J, Glockner FO. The SILVA ribosomal RNA gene database project: improved data processing and web-based tools. *Nucleic Acids Res*. 2013:**41**(D1):D590–D596. https://doi.org/10.1093/nar/gks1219.

Romero P, Obradovic Z, Li X, Garner EC, Brown CJ, Dunker AK. Sequence complexity of disordered protein. *Proteins*. 2001:**42**(1):38–48. https://doi.org/10.1002/1097-0134(20010101)42:1<38::AID-PROT50>3.0.CO;2-3.

Schmidt TM, Relman DA. Phylogenetic identification of uncultured pathogens using ribosomal RNA sequences. *Methods Enzymol*. 1994:**235**:205–222. https://doi.org/10.1016/0076-6879(94)35142-2.

Sillitoe I, Dawson N, Lewis TE, Das S, Lees JG, Ashford P, Tolulope A, Scholes HM, Senatorov I, Bujan A, *et al*. CATH: expanding the horizons of structure-based functional annotations for genome sequences. *Nucleic Acids Res*. 2019:**47**(D1):D280–D284. https://doi.org/10.1093/nar/gky1097.

The RNAcentral Consortium. RNAcentral: a hub of information for non-coding RNA sequences. *Nucleic Acids Res*. 2019:**47**(D1):D1250–D1251. https://doi.org/10.1093/nar/gky1206.

Toledo-Patino S, Chaubey M, Coles M, Hocker B. Reconstructing the remote origins of a fold singleton from a flavodoxin-like ancestor. *Biochemistry*. 2019:**58**(48):4790–4793. https://doi.org/10.1021/acs.biochem.9b00900.

Tompa P. Intrinsically disordered proteins: a 10-year recap. *Trends Biochem Sci*. 2012:**37**(12):509–516. https://doi.org/10.1016/j.tibs.2012.08.004.

Toto A, Sormanni P, Paissoni C, Uversky VN. Editorial: intrinsically disordered proteins and regions: the challenge to the structure-function relationship. *Front Mol Biosci*. 2022:**9**:962643. https://doi.org/10.3389/fmolb.2022.962643.

Uversky VN. Dancing protein clouds: the strange biology and chaotic physics of intrinsically disordered proteins. *J Biol Chem*. 2016:**291**(13):6681–6688. https://doi.org/10.1074/jbc.R115.685859.

Wadi L, Reinke AW. Evolution of microsporidia: an extremely successful group of eukaryotic intracellular parasites. *PLoS Pathog*. 2020:**16**(2):e1008276. https://doi.org/10.1371/journal.ppat.1008276.

Wang HC, Xia X, Hickey D. Thermal adaptation of the small subunit ribosomal RNA gene: a comparative study. *J Mol Evol*. 2006:**63**(1):120–126. https://doi.org/10.1007/s00239-005-0255-4.

Warrenfeltz S, Basenko EY, Crouch K, Harb OS, Kissinger JC, Roos DS, Shanmugasundram A, Silva-Franco F. EuPathDB: the eukaryotic pathogen genomics database resource. *Methods Mol Biol*. 2018:**1757**:69–113. https://doi.org/10.1007/978-1-4939-7737-6_5.

Woese CR, Fox GE. Phylogenetic structure of the prokaryotic domain: the primary kingdoms. *Proc Natl Acad Sci U S A*. 1977:**74**(11):5088–5090. https://doi.org/10.1073/pnas.74.11.5088.

Wright PE, Dyson HJ. Intrinsically disordered proteins in cellular signalling and regulation. *Nat Rev Mol Cell Biol*. 2015:**16**(1):18–29. https://doi.org/10.1038/nrm3920.

Xu D, Zhang Y. Ab initio structure prediction for *Escherichia coli*: towards genome-wide protein structure modeling and fold assignment. *Sci Rep*. 2013:**3**(1):1895. https://doi.org/10.1038/srep01895.

Zuker M. Mfold web server for nucleic acid folding and hybridization prediction. *Nucleic Acids Res*. 2003:**31**(13):3406–3415. https://doi.org/10.1093/nar/gkg595.